Supplemental Material

Projecting Excess Mortality in 2030 with Spatially-Varying Ozone-Temperature Risk Surfaces

Ander Wilson[1], Brian J. Reich[2], Christopher G. Nolte[3], Tanya L. Spero[3],
Bryan Hubbell[4] and Ana G. Rappold[5]

Data Calibration

Both the NMMAPS data and the regional climate and air quality modeling contain data representative of the years 1995 to 2000. We calibrated the modeled temperature and ozone data from WRF and CMAQ to ensure that the distributions were the same for that overlap period in each city while preserving the projected changes between time periods. To calibrate the ozone data we treated the square root of MDA8 ozone as normal and matched the mean and standard deviation of the observed and modeled data for the overlap period. We calculated the mean (μ_c) and standard deviation (σ_c) of the square root of the ozone in the CMAQ data for the overlap period and the mean (μ'_c) and standard deviation (σ'_c) of the square root ozone in the NMMAPS data for the same time period. We then transformed the raw CMAQ ozone data x^*_{1ct} for city c on day t for each day in both the 1995-2005 and 2025-2035 time periods as

$$x_{1ct} = \left[\max\left\{\left(\frac{\sqrt{x^*_{1ct}} - \mu_c}{\sigma_c}\right)\sigma'_c + \mu'_c, 0\right\}\right]^2.$$

Both time periods were scaled by the same amount to preserve the between-time-period changes in projected ozone and temperature values.

Because ozone cannot be negative, we place a minimum value of 0 on the calibrated root ozone before squaring. There were 16 total days across all cities and years with negative transformed ozone values on square root scale, and the smallest is -2.16. We calibrated temperature on its original scale using the same method, but allowed for negative values. One city, Muskegon, Michigan, did not have NMMAPS ozone data in the overlap period, so we used NMMAPS ozone data from 1987 through 1991 for this city. This calibration is also necessary to calibrate the distribution to the same scale as MDA8 calculated from NMMAPS hourly trimmed data. Supplemental Figure S1 compares the distribution of temperature and ozone in the CMAQ and NMMAPS data. Figure 1 compares the distribution of ozone in the calibrated CMAQ data for the two time periods.

Confounder Model

The confounder model includes age-specific intercepts (less than 65, 65-74, 75 and over), categorical variables for day of week, and smooth functions of time interacted with age group with seven degrees of freedom per year constructed with natural splines. Additional effects of weather are controlled for with natural cubic spline of the 3-day running mean of temperature with six degrees of freedom, natural cubic spline of dew point with three degrees of freedom, and of the 3-day running mean of dew point with three degrees of freedom.

Second-Stage Computation

We estimated the risk surfaces using the NMMAPS data with ten independent Monte Carlo Markov chains of length 1,000,000. We discarded the first 500,000 for burn-in and thinned the posterior by keeping every 100th draw to get a posterior sample size of 5,000 for each of the ten chains. We then combined the ten posterior samples into a single posterior sample of size 50,000. Convergence was assessed by inspecting trace and autocorrelation plots and comparing the stability of the estimates across the ten independent chains prior to combining them. The model was determined to have converged during burn-in. The estimates of EM and EMR are calculated separately for each of the 50,000 posterior draws retained for analysis and used to calculate the posterior mean, standard deviation, and credible intervals of each estimate.

Figure S1: Calibration plots showing the quantiles of daily mean temperature (top) and daily MDA8 ozone (bottom) and for the current and future time periods as well as the calibration period from the modeled and NMMAPS data.

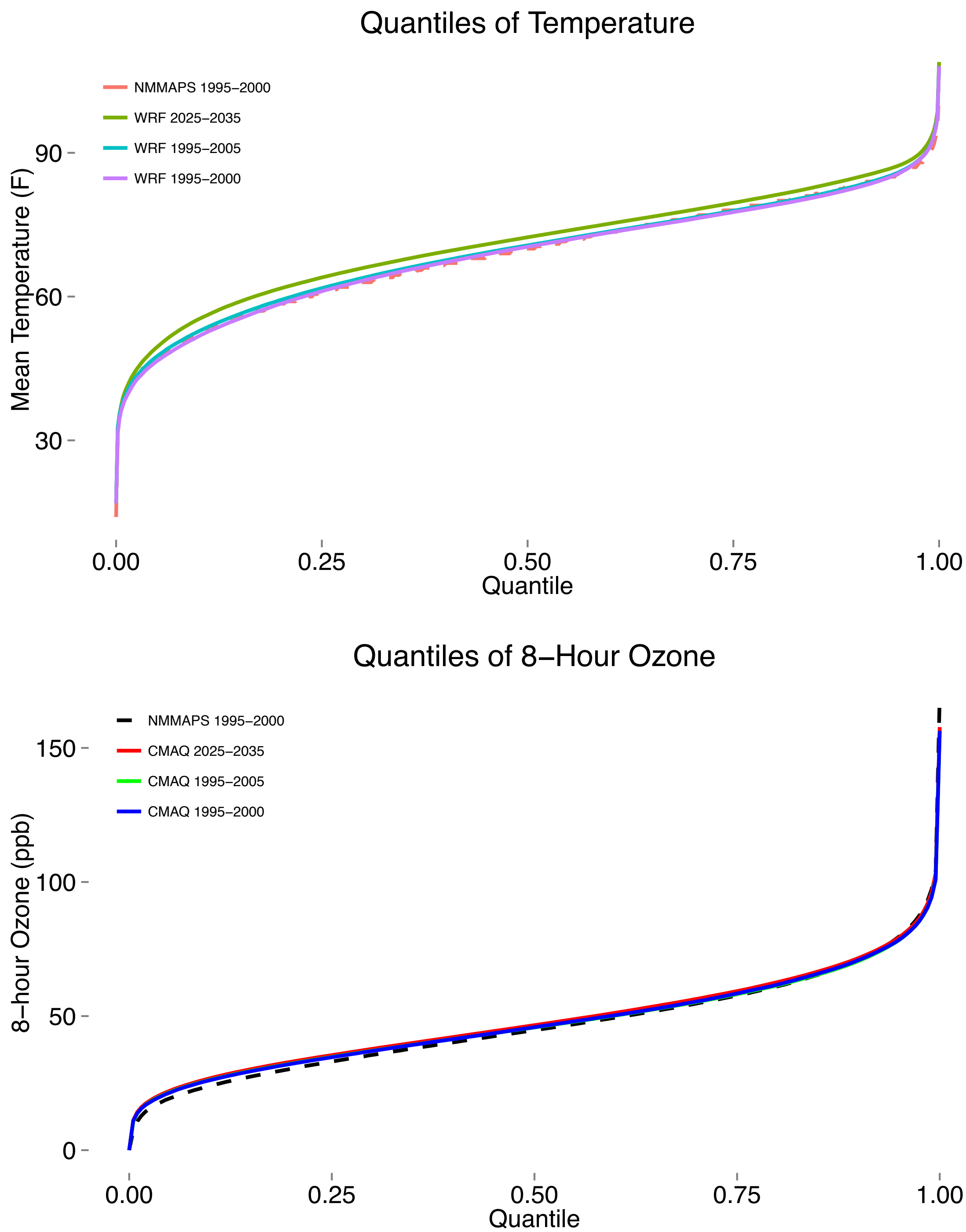

Figure S2: Summary of the shift in MDA8 ozone distribution from 1995-2005 to 2025-2035. For each time period, the mean number of days per city-year with ozone exceeding each ozone concentration is shown.

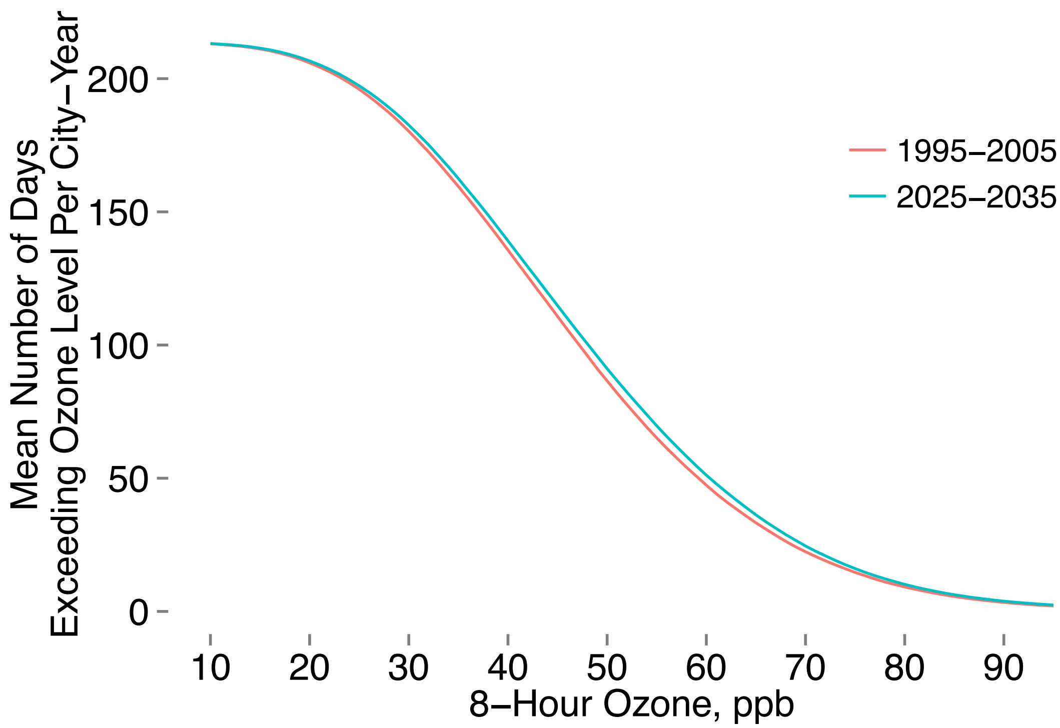

Figure S3: Change in excess mortality rate (red) per 100,000 persons with 95% credible regions (black) attributed to ozone levels above 75 ppb. This is the same as Figure 2b in the text with intervals included. Regions and cities follow Samet et al. (2000a,b).

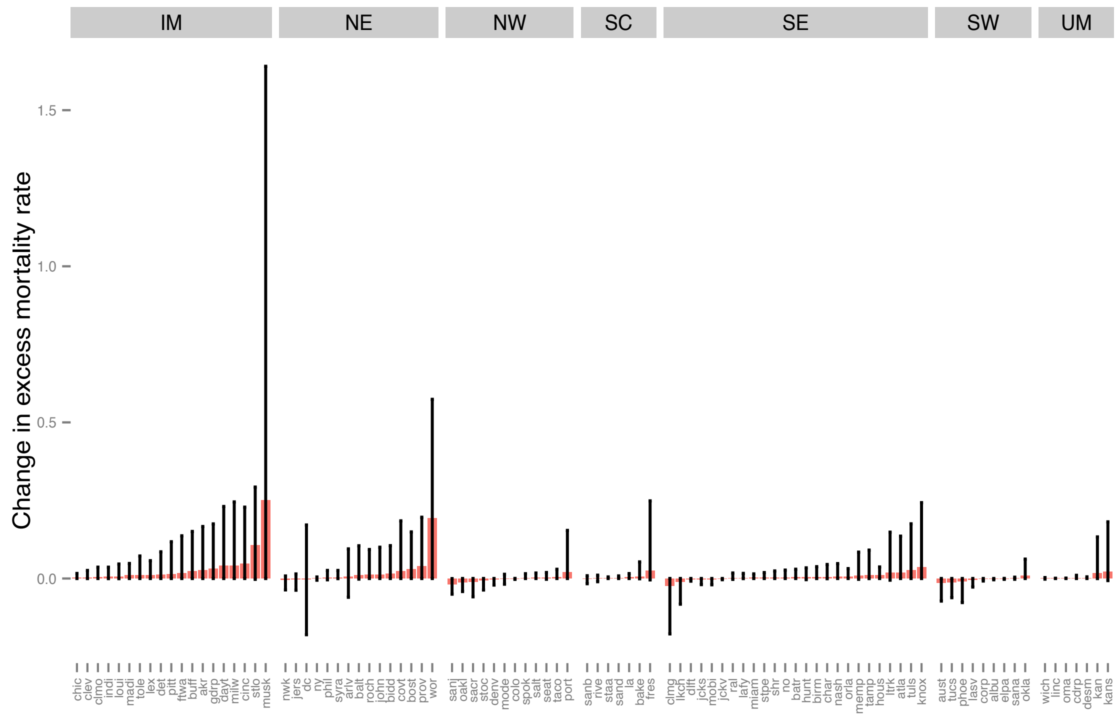

Figure S4: Excess ozone related mortality by region attributed to ozone exceeding 40 ppb (top) and exceeding 75 ppb (bottom).